

²⁷Al MQ-MAS NMR as a Tool for Structure Determination in Nanocomposite Materials: The Nature of Al Pillars in “Al₁₃–heidi” Pillared Clays

Jean-Baptiste d’Espinose de la Caillerie* and Pascal P. Man

Laboratoire de Physique Quantique et Laboratoire de Chimie des Surfaces, FRE CNRS 2312, Ecole Supérieure de Physique et de Chimie Industrielles de la Ville de Paris, 10 rue Vauquelin, 75231 Paris Cedex 05, France

Miguel Angel Vicente† and Jean-François Lambert

Laboratoire de Réactivité de Surface, UMR CNRS 7609, Université Pierre et Marie Curie, case courrier 178, 4 place Jussieu, 75252 Paris Cedex 05, France

Received: November 1, 2001

²⁷Al 3QMAS 2D NMR was used to study the molecular-level organization of a clay pillared with the “Al₁₃–(heidi)₆³⁺” polycation, whose unusual structure is stabilized by hydroxyethyliminodiacetate (heidi) ligands. The quadrupolar line shape and the isotropic chemical shifts were first unambiguously determined on a solid salt of the polycation. This compound was then used to identify the fingerprint of the Al₁₃(heidi)_x³⁺ polycation in a sample of saponite clay that had been intercalated with a solution containing Al(III) and heidi ligands, showing that the basic structure of the Al polymer had been preserved upon intercalation. A more detailed analysis of 3QMAS 2D NMR line shapes indicated, however, that a selective partial hydrolysis reaction had occurred, most probably leading to Al₁₃(heidi)₃³⁺ polycations (loss of three heidi ligands). Thus, 3QMAS NMR allowed to choose one structural model for these nanocomposites from the several compatible with previously published characterizations.

Introduction

The recent developments in solid-state nuclear magnetic resonance (NMR), especially for quadrupolar nuclei, have considerably increased the potential of this technique for the elucidation of the molecular structure of materials. This is especially true for nanocomposite materials. Such materials consist of the intermingling of two or more constituents of nanometer-size dimensions and well-defined molecular structure. The organization of the different constituents, however, may not result in a well-defined 3-dimensional periodicity, thus making diffraction methods inapplicable. A typical example is provided by aluminum-pillared clays: the clay layers are less than 1 nm thick (although they are much more extended in the other two directions), and they are held apart by inorganic polymers with a diameter in the nanometric range.¹ There is usually a well-defined periodicity in the direction perpendicular to the layers (*c* axis), but not in the *a* and *b* directions. For some time after the discovery of these materials, X-ray diffraction failed to resolve the structure of the Al-containing pillars. One of the early successes of one-pulse ²⁷Al NMR was to conclusively demonstrate that the pillars consist of tridecamers with formula [Al₁₃O₄(OH)₂₄(H₂O)₁₂]⁷⁺ having the so-called “ε-Keggin” structure (later called Al₁₃–Keggin).²

This success was not repeated for related materials pillared with Al or other elements for at least two reasons: one a consequence of the empirical nature of clay pillaring procedures, and the other an intrinsic limitation of the technique. First, effective clay pillaring has usually been the result of a blind

optimization of synthesis parameters, rather than based on a previous sound understanding of the chemistry implied. It has been realized from the beginning that the first step in pillaring consists of the intercalation of bulky polycations by ion exchange of the original compensating cations of the clay matrix in contact with an aqueous solution, but seldom has much effort been directed at characterizing the structure of the preexisting polycations in solution. As a result, many pillared clays are probably inhomogeneous systems containing a mixture of different polycations.

Second, although NMR is in principle very sensitive to the chemical environment of the target nucleus, several factors may limit its resolution in practical cases. Anisotropy of the NMR signal results in its spreading over a wide spectral region, compromising the identification of chemical species. It is usually present in the solid phase and may even be limiting in the liquid phase for such bulky species as Al₁₃–Keggin, which are not mobile enough to be motionally averaged in normal conditions. Indeed, the early identification of the latter species relied on the observation of its central Al, which happens to be in a highly symmetrical environment, whereas the other 12 Al nuclei of the polycation remained hardly observable.

For solid samples, the technique of magic angle spinning (MAS) was designed to average signal anisotropy. Sharp MAS NMR signals are indeed observed for nuclei with spin *I* = 1/2, which are only submitted to chemical shift and dipole–dipole interactions, but in the case of ²⁷Al (*I* = 5/2), additional quadrupolar interactions are present and are not completely averaged out by MAS. As a result, ²⁷Al NMR spectra provide information essentially on the first coordination sphere of the Al(III) ion (whereas NMR of ¹H, ¹³C, or even ¹⁹⁵Pt gives access to longer-range environment). One may easily distinguish

* To whom correspondence should be addressed. Phone: (33) 01 40 79 46 20. Fax: (33) 01 40 79 47 44. E-mail: Jean-Baptiste.Despinose@espci.fr

† Present address: Departamento de Química Inorgánica, Facultad de Ciencias Químicas, Plaza de la Merced s/n, 37008 Salamanca, Spain.

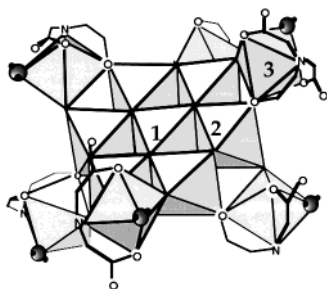


Figure 1. Structure of the Al_{13} -heidi-Cl polycation. There are three nonequivalent octahedral environments for the thirteen Al(III) . It consists of a core which can be seen as a portion of an hexagonal layer with a central AlO_6 site (type 1) sharing edges with six peripheral AlO_6 sites (type 2). This is completed by a shell of six AlO_5N sites coordinated with an heidi ligand (type 3).

between (AlO_4) and (AlO_6) coordination spheres (corresponding to tetrahedral $^{\text{IV}}\text{Al}$ and octahedral $^{\text{VI}}\text{Al}$, respectively), but it is generally impossible to determine the connections between Al-containing polyhedra, as would be necessary for unravelling polycation structures.

Over the past decade, the quadrupolar multiple quantum MAS (MQMAS) technique has been developed precisely to obviate this difficulty.³ It is a 2-dimensional technique, that basically disentangles quadrupolar from chemical-shift interactions by observing them differently along two different directions in the frequency domain.⁴ It has now well demonstrated its potential in studies of model compounds but also for the resolution of structural problems of practical significance.

The present work constitutes an attempt to apply ^{27}Al MQMAS to the structural elucidation of a new class of pillared clays, whose preparation has been described in a previous publication.⁵ In contrast to the common practice, we used an intercalating solution containing a well-defined polycation with a structure different from the usual Al_{13} -Keggin. The structure of this polycation is depicted in Figure 1. It is stabilized by six hydroxyethyliminodiacetate (heidi) ligands and, therefore, will be denoted as Al_{13} -heidi. It is easily obtained in aqueous solutions,⁶ and contact of such solutions with saponite clays resulted in the intercalation of bulky species between the clay layers. Converging circumstantial evidence suggested that these species were unmodified Al_{13} -heidi polycations. The direct structure elucidation by diffraction methods was, however, impossible, so that the success of the synthetic approach could not be fully established. As we will show, MQ-MAS results now allow us to confirm the nature of the pillaring species and advance hypotheses on the nature of its chemical transformations upon pillaring.

Experimental Section

Materials and Synthesis Procedures. Preparation of the Al_{13} -heidi polycations was carried out along the method of Moore et al.^{6,7} $\text{AlCl}_3 \cdot 6\text{H}_2\text{O}$ and (heidi) ligands (Acros Organics, 98%) were dissolved in deionized water with Al:heidi ratios of 2.0 or 3.0. Crystals of the chloride salt of the Al_{13} -heidi polycations could be precipitated from the solution. They will be denoted as Al_{13} -heidi-Cl.

A solution with Al:heidi ratio of 2.0 was contacted with a suspension of Ballarat saponite (12 g L^{-1} ; natural clay provided by the Clay Minerals Repository, University of Missouri, standard purification procedures), using an Al:clay ratio of 20 mmol g^{-1} . After 24 h under stirring, the suspension was

centrifuged; the solid phase was redispersed in water, washed four times by dialysis, and then dried in air at 50°C . The optimization of the preparation procedure is discussed in the literature together with the detailed characterization of the obtained solids.⁵ Powder X-ray diffraction on the sample selected for the present study showed an intense line corresponding to a d spacing of 25.3 \AA , which was assigned to the (001) family of planes; second- and third-order peaks were also observable. In comparison with the d_{001} value in the starting saponite (14.8 \AA), this shows that the applied procedure had resulted in the intercalation of bulky species between the clay layers. The surface area was low ($25 \text{ m}^2 \text{ g}^{-1}$), indicating clogging of the interlayer space, but could be increased to $350 \text{ m}^2 \text{ g}^{-1}$ by calcination. The uncalcined intercalated sample will be denoted as IntSap.

MAS NMR. Magic angle spinning nuclear magnetic resonance (MAS NMR) experiments were performed on a Bruker ASX500 spectrometer at 11.7 T in 4 mm zirconia rotors. ^{27}Al one-pulse experiments were performed spinning at 14 kHz with a selective pulse ($< \pi/12$) duration of $0.5 \mu\text{s}$, recycle time 1 s , and 5000 acquisitions.

The triple quantum MAS (3QMAS) spectra were acquired with Z-filtering⁸ and hypercomplex (States) phase detection. The pulse durations were set empirically to 3 and $1 \mu\text{s}$ for the first and the second pulse, respectively ($\Omega_1/2\pi = 132 \text{ kHz}$), and to $3 \mu\text{s}$ for the third selective pulse ($\Omega_2/2\pi = 26 \text{ kHz}$). These values maximized the observed signal. $256 t_1$ increments of 16 and $5 \mu\text{s}$ for Al_{13} -heidi-Cl and IntSap respectively were acquired in the first dimension. A total of 480 scans were accumulated with a recycle time of 1 s . Data processing including zero filling, shearing, and scaling according to convention⁹ C_Z were performed using Grandinetti's RMN program.¹⁰

Results and Discussion

Solid Salt. The ^{27}Al one-pulse MAS NMR spectrum of the solid salt Al_{13} -heidi-Cl reveals the complex response of the superimposed first-order quadrupolar line shapes corresponding to the expected three nonequivalent aluminum sites (Figure 2a). In principle, the resonance of each site is fully determined by its isotropic chemical shift ($\delta_{\text{CS}}^{(\text{iso})}$), quadrupolar coupling constant (C_Q), and asymmetry parameter (η); but the one-pulse spectrum has insufficient resolution to allow unequivocal assignments of the parameters for all three sites by blind fitting of the line shape.

In contrast, the 3QMAS two-dimensional spectrum (Figure 3a) clearly separates the contributions from the three aluminum sites. Furthermore, it allows us to evaluate the characteristic NMR parameters of each Al site. From the observed chemical shifts of the center of gravity of the resonance in the F_1 ($\delta_{\text{G1}}^{(\text{obs})}$) and F_2 ($\delta_{\text{G2}}^{(\text{obs})}$) dimensions, the true isotropic chemical shift is deduced from

$$\delta_{\text{CS}}^{(\text{iso})} = \frac{10}{27} \delta_{\text{G2}}^{(\text{obs})} - \frac{4}{9} \delta_{\text{G1}}^{(\text{obs})}$$

The quadrupolar coupling constant and the asymmetry parameter cannot be obtained independently, but the parameter

$$C_{Q\eta} = \frac{e^2 q Q}{h} \sqrt{\frac{\eta^2}{3} + 1}$$

TABLE 1

MQMAS (2D)				one-pulse (1D) ^a						
$\delta_{G1}^{(obs)}$ ±2 ppm	$\delta_{G2}^{(obs)}$ ±2 ppm	$\delta_{CS}^{(iso)}$ ±2 ppm	$C_{Q\eta}$ ±0.3 MHz	$\delta_{CS}^{(iso)}$ ±0.5 ppm	ν_Q ±0.05 MHz	η	$C_{Q\eta}$	exponential broadening	amplitude ±3%	assignment
-41 ppm	13 ppm	23 ppm	5.3 MHz	25.0 ppm	0.70 MHz	0.83	5.2 MHz	8 Hz	42%	type 3
-28 ppm	-2.5 ppm	11.5 ppm	6.3 MHz	12.5 ppm	0.89 MHz	0.38	6.0 MHz	15 Hz	51%	type 2
-20 ppm	10 ppm	12.5 ppm	2.7 MHz	12.0 ppm	0.36 MHz	0	2.4 MHz	40 Hz	7%	type 1
-91 ppm	67 ppm	64.5 ppm	0.0 MHz	66 ppm					19%	Al ^{IV} in clay

^a The accuracy of the parameters of the fit are difficult to evaluate. They are given for $\delta_{CS}^{(iso)}$ and ν_Q as the bounds outside of which, whatever the values of the amplitudes, the broadening, and η , a fit is impossible.

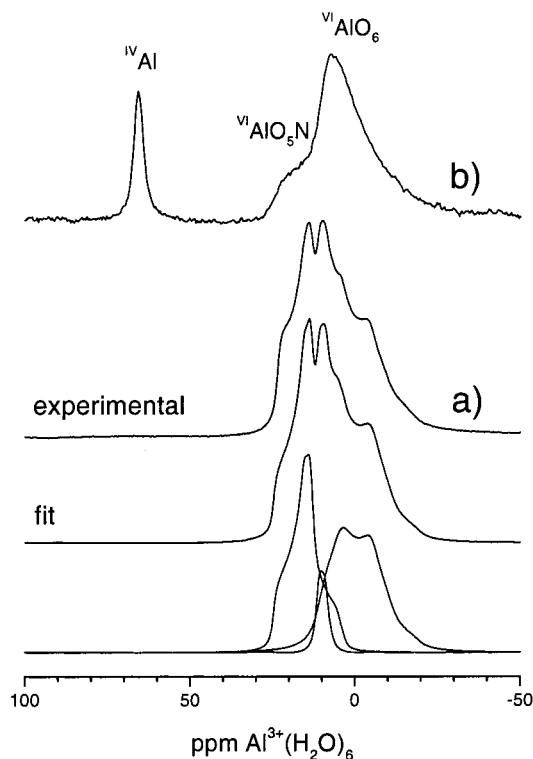


Figure 2. One-pulse ²⁷Al MAS NMR spectra. (a) Solid salt Al₁₃–heidi–Cl: an excellent fit is obtained for the 1D line shapes using the 3QMAS data (Table 1). (b) Intercalated saponite: besides the ^{IV}Al resonance of the saponite layer, the ^{VI}Al resonance line shape shows that the Al₁₃–heidi polycation is modified upon intercalation. In particular, the decrease of the ^{VI}AlO₅N resonance reflects the loss of half the heidi ligands.

commonly used for characterizing a material can be determined from⁹

$$C_{Q\eta} = \frac{I(2I-1)\omega_0}{2\pi} \sqrt{\frac{40}{3[I(I+1)-3/4]}} \sqrt{-4/9[\delta_{G1}^{(obs)} + 17/12\delta_{G1}^{(obs)}]}$$

In the present case, the center of gravity of the resonances can only be obtained with an accuracy of ±2 ppm, leading to approximate values of $\delta_{CS}^{(iso)}$ and $C_{Q\eta}$ (Table 1). The quadrupolar parameters are sometimes determined by direct line shape analysis of F_2 projections of F_1 resolved resonances. In the present case, consequent broadening, not to speak of overlap, in the isotropic F_1 dimension precludes full determination of the quadrupolar parameters by this method.¹¹ To avoid lengthy debate of this question, the 1D spectrum was fitted using the values and the accuracies obtained from 2D MQMAS with the

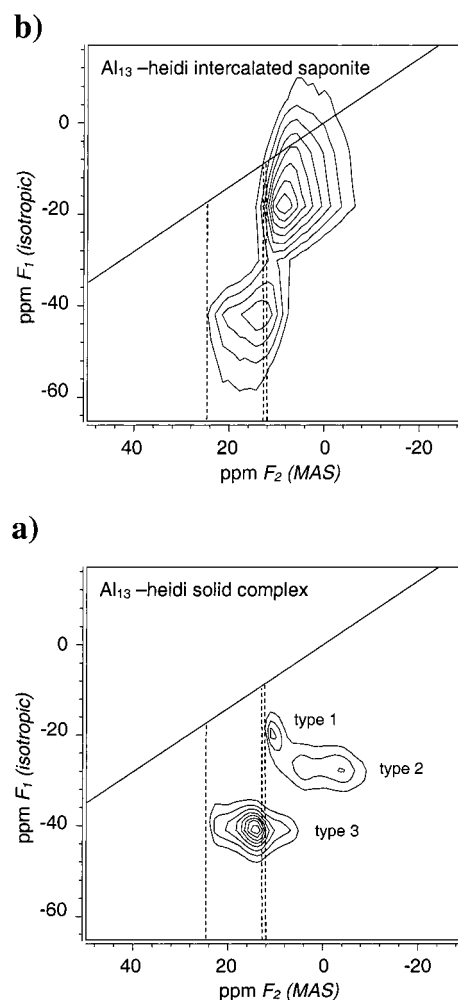


Figure 3. Sheared ²⁷Al ($I = 5/2$) 3QMAS spectra (octahedral resonances region). Contour lines are drawn every 10% starting at 20% of the maximum. The null quadrupolar lines are drawn (dotted $\delta_{CS}^{(iso)} = \delta_{G2}^{(obs)}$, solid $\delta_{G1}^{(obs)} = -17/12\delta_{G2}^{(obs)}$). (a) Solid salt Al₁₃–heidi–Cl: the three maxima are attributed to the three types of ^{VI}Al environments on the basis of subsequent fitting of the 1D line shapes (Figure 2a) constrained by the 2D 3QMAS data (Table 1). (b) Intercalated saponite: only two maxima are visible due to increased dipolar broadening as shown by the crossing of the null quadrupolar line $\delta_{G1}^{(obs)} = -17/12\delta_{G2}^{(obs)}$.

constraints:

$$\delta_{CS}^{(iso)}(1D) = \delta_{CS}^{(iso)}(2D) \pm 2 \text{ ppm}$$

$$C_{Q\eta}(1D) = C_{Q\eta}(2D) \pm 0.3 \text{ MHz}$$

$$C_{Q\eta}(1D) = \frac{2I(2I-1)\nu_Q(1D)}{3} \sqrt{\frac{\eta(1D)^2}{3} + 1}$$

with

$$\nu_Q = \frac{e^2 q Q}{h} \frac{3}{2I(2I-1)}$$

In addition, considering that the electrical field gradient for site 1 is axially symmetric, one of the asymmetry parameter is set to zero. The added advantage in proceeding this way is that the relative amplitude of each resonance can be obtained quantitatively from the 1D spectrum, whereas this information is much more delicate to recover from a 2D MQMAS spectrum where efficiency of the MQ excitation requires sophisticated experiments.¹² The NMR parameters obtained in this way (Table 1) provide a very satisfactory fit of the resonance of the Al₁₃-heidi-Cl salt, as can be seen by comparison of the fit with the experimental line shape (Figure 2a).

It is then possible to assign the three observed resonances to the three aluminum sites expected in the polycation. The first resonance is the only one with an isotropic chemical shift lying in the range expected for a AlO₅N coordination and is therefore assigned to the type three aluminum. We note that the $\delta_{CS}^{(iso)}$ value obtained is identical to the one measured for the type three aluminum of the Al₂-heidi dimer in solution.⁶ The electrical field gradient at this position is expected to differ markedly from axial symmetry because type three aluminum is coordinated to five chemically inequivalent oxygens, and indeed, this chemical shift corresponds to the resonance with the highest asymmetry parameter. Conversely, the third resonance with $\eta = 0$ is assigned to the central type one aluminum with full axial symmetry. The chemical shift of this resonance, as well as that of the second resonance, are in the range of an AlO₆ coordination. Finally, the second resonance is assigned by default to the type two aluminum with an intermediate asymmetry parameter. The values of $C_{Q\eta}$ and η for this resonance are reasonably close to what has been previously measured by nutation NMR for the octahedral sites of the Keggin Al₁₃ polycation.¹³ This assignment for the three resonances is further supported by considering the amplitudes of the three resonances, which were not constrained at all during the fit. They are reasonably close to the theoretical ratio of 46%:46%:8%. It is also remarkable that the line width decreases from type one to type three aluminum resonances. Generally speaking, the line width of a second-order quadrupolar line shape results from a superposition of inhomogeneous (distribution of environments resulting in a distribution of chemical shift and quadrupolar parameters, residual chemical shift anisotropy) and homogeneous (dipolar coupling) broadenings and is thus difficult to interpret directly from the one-pulse spectra. However, analysis of the shape of the 3QMAS correlation resonances provides additional information on the physical origin of the broadening.¹⁴ Considering that the line shapes are distorted because of the shearing and because of uneven MQ transfer efficiency across the distribution of quadrupolar interaction, only qualitative observations are relevant here.¹¹ First, the relative importance of a distribution of chemical shifts versus a distribution of quadrupolar interactions can be estimated from the shape of the contour lines: dispersion of second-order quadrupolar interaction extends the resonance perpendicularly to the null quadrupolar line $\delta_{G1}^{(obs)} = -17/12\delta_{G2}^{(obs)}$, whereas distribution of chemical shift results in an extension along the $\delta_{G1}^{(obs)} = -17/12\delta_{G2}^{(obs)}$ line and across the $\delta_{CS}^{(iso)} = \delta_{G2}^{(obs)}$ line. Second, residual distortion of the 2D contours after shearing indicates a contribution of homogeneous, i.e., dipolar, interaction to the broadening.¹¹ Furthermore, a crossing of the null

quadrupolar line $\delta_{G1}^{(obs)} = -17/12\delta_{G2}^{(obs)}$ can only result from a homogeneous broadening. Here, the 3Q resonances of the Al₁₃-heidi-Cl salt (Figure 3a) do not extend significantly along $\delta_{G1}^{(obs)} = -17/12\delta_{G2}^{(obs)}$ or across $\delta_{CS}^{(iso)} = \delta_{G2}^{(obs)}$, which indicates that the dispersion of resonances is not predominantly due to chemical shift distribution. There is no indication either of extension perpendicularly to $\delta_{CS}^{(iso)} = -17/12\delta_{G2}^{(obs)}$, that is of the dispersion of quadrupolar interaction. In addition, a slight distortion of the contours is perceptible establishing the occurrence of dipolar broadening. In conclusion, the MQMAS experiment establishes indirectly that the broadening is mostly dipolar. In further support of our assignment, one should therefore note that the line broadening of the resonances of the three Al sites in the one-pulse spectrum increases with the increasing number of hydroxyl ligands, that is, with an increasing number of immobile protons strongly coupled to aluminum by homogeneous dipolar interactions.

In summary, the conjunction of 1D one-pulse and 2D 3QMAS NMR data allows a precise assignment of the resonances of the three types of aluminum in terms of isotropic chemical shift, quadrupolar, and, to a lesser extent, dipolar interactions. It must be emphasized that, notwithstanding the structural information provided by the quadrupolar parameters themselves, the true $\delta_{CS}^{(iso)}$ could not have been obtained without determining first the quadrupolar line shape.

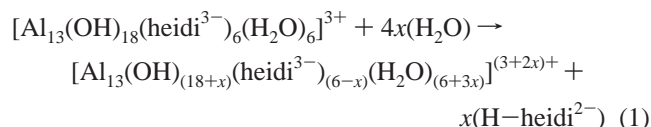
Intercalated Saponite. Let us now consider the one-pulse spectrum of the intercalated saponite IntSap (Figure 2b). It exhibits a resonance at 66 ± 0.4 ppm, i.e., in the range of ^{IV}Al, that is ascribable to (AlO₄) tetrahedra in the clay layer. The rest of the spectrum consists of a resonance in the chemical shift range of ^{VI}Al with a maximum at 7 ± 1 ppm and a shoulder around 25 ppm. These features must be due to intercalated Al, because Ballarat saponite has no octahedrally coordinated Al in its layers. At first sight, they are reminiscent of the spectrum of Al₁₃-heidi, suggesting that the polymer present in the solution has actually been intercalated. There are nonetheless significant differences: the type three Al of Al₁₃-heidi-Cl gives a strong contribution at 14.5 ppm which is not observed in the intercalated sample, and in general, although the resonance is not overall broader, the spectral singularities of the quadrupolar line shapes have disappeared in IntSap.

This aspect of the spectrum could be interpreted in three ways. The first hypothesis would be to consider that intact polycations are intercalated but that structural distortions are somehow induced by the electrostatic interaction with the clay layers. The second would be to accept that the polycation is partly hydrolyzed in a way that decreases the N:Al ratio, whereas the third would be to consider that the polycation is partly depolymerized so that other aluminic species are present in the interlayers together with Al₁₃-heidi, and the signal in the octahedral Al region is of a composite nature.

The first proposition (polymer distortions by local constraints) is an easy way out of the difficulties in spectrum interpretation: the lack of resolved singularities would then be due to the resulting dispersion of chemical shifts and quadrupolar interactions. However, quantitative analysis seems to rule this out, for the shoulder at 25 ppm, corresponding to Al in (AlO₅N) coordination, can only account for a proportion of about 17 (± 5)% of the total octahedral aluminum, whatever the quadrupolar line shape adopted, as opposed to 46% in the original Al₁₃-heidi. The decrease of this type of coordination requires the loss of about one-half of the heidi ligands from the species initially present in the intercalating solution. This conclusion, derived from one-pulse NMR, is confirmed by simple elemental

analysis: the (N/intercalated Al) molar ratio in IntSap is 0.29, instead of the expected value of 0.46 for the intercalation of intact Al₁₃–heidi polycations.⁵

It is thus necessary to reject intercalation of the polycation as such and to consider the various possibilities for hydrolysis reactions (the second hypothesis). As mentioned in our previous study,⁵ polycation hydrolysis could be written as a simple aquation, with the release of a fraction of the heidi ligands:



where x would be treated as an adjustable parameter in order to justify the experimentally observed elemental ratio.

As such, this looks like an ad hoc assumption, because (H–heidi^{2–}) ligands have a strong affinity for aluminum, so that one expects eq 1 to be displaced to the left in solution. Therefore, one cannot rule out the third hypothesis, that is, that the decomposition of the polymeric complex leads to a distribution of oxo-hydroxo species with lower molecular weight. The observed ²⁷Al NMR spectrum would then result from the superimposition of at least two contributions: that of the remaining intercalated Al₁₃–heidi complex and those of depolymerized oxo-hydroxo species. Candidate structures for the latter can be proposed from ²⁷Al liquid NMR studies⁶ and would include [Al(H₂O)₆]³⁺, [Al(H₂O)₅(OH)]²⁺, and the dimer [Al₂(H₂O)₈(OH)₂]⁴⁺. The neutral dimer [Al₂(heidi^{3–})₂(H₂O)₂]⁰ has also been evidenced in solution studies, but it is not expected to be intercalated in the clay because it bears no positive charge. Besides, it would result in an increase of the number of Al in (AlO₅N) environments, not a decrease as observed.

Whatever hypothesis we retain should be compatible with global electroneutrality: the negative charge of the clay layers, which is constant, should be compensated by the cumulative charge of all of the Al species present in the interlayer. Now, the (fixed Al/layer charge) molar ratio, estimated from elemental analysis, is equal to 4.3.⁵ As it turns out, the quantification of the NMR data can provide an independent estimate of the (fixed Al/layer charge) ratio. As we have said, the octahedrally coordinated Al (V^IAl) corresponds only to Al in intercalated species in this material; on the other hand, each tetrahedrally coordinated Al (V^{IV}Al) gives rise to one substitutional electric charge in the clay layer. Therefore, one obtains:

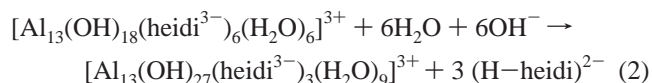
$$(\text{fixed Al/layer charge}) = \text{V}^{\text{I}}\text{Al}/\text{V}^{\text{IV}}\text{Al} = 5.3$$

not too different from the estimate based on chemical analysis. Both estimates are quite high and close to the ($n_{\text{Al}}/\text{positive charge}$) ratio of the intact [Al₁₃(OH)₁₈(heidi^{3–})₆(H₂O)₆]³⁺ polymer, which is 13:3, that is, 4.33. In contrast, the corresponding ratios for depolymerized species are much lower: 0.33 for [Al(H₂O)₆]³⁺ and 0.5 for [Al(H₂O)₅(OH)]²⁺ and [Al₂(H₂O)₈(OH)₂]⁴⁺. This argument is not sufficient to rule out the depolymerization hypothesis, however, because our knowledge of Al aqueous chemistry is still imperfect and other species may be present.

3QMAS NMR actually provides another source of information relevant for this question. As seen on Figure 3b, the responses are considerably broadened after intercalation as compared to the bulk salt, and the types one and two aluminum sites are not resolved after intercalation, a feature that was already observed in the 1-D spectra. Interestingly, the 3QMAS resonance of the AlO₆ sites crosses the null quadrupolar line, a

feature that was not observable in the Al₁₃–heidi–Cl salt. This is important because it indicates homogeneous broadening (dipolar in origin), as opposed to heterogeneous broadening (the superimposition of signals with variable chemical shifts due to a distribution of chemical environments) which would not account for the crossing of the null quadrupolar line. Now, if we look at the partly aquated Al₁₃ polymers resulting from reaction 1, we see that aquation results in an increase in the number of protons in close vicinity of the Al nuclei (because of new (OH) and (H₂O) ligands), which induces increased dipolar broadening. On the other hand, depolymerization of Al₁₃ could also result in increased dipolar broadening but would have translated additionally in a distribution of Al chemical environments, inducing an heterogeneous broadening with the crossing of the $\delta_{\text{CS}}^{(\text{iso})} = \delta_{\text{G2}}^{(\text{obs})}$ line and an elongation along the $\delta_{\text{CS}}^{(\text{iso})} = -17/12\delta_{\text{G2}}^{(\text{obs})}$ line. Such features are not observed here. Thus, the shape of the 3-Q MAS resonance favors hypothesis 2 (aquation without depolymerization) over hypothesis 3 (intercalation of different, partly depolymerized Al species).

In summary, the NMR data suggest the intercalation of an Al₁₃(heidi)₃³⁺ complex derived from the Al₁₃(heidi)₆³⁺ in solution. This still leaves some questions open. The first concerns the global charge of the postulated Al₁₃(heidi)₃ entities. For reasons of global electroneutrality, a 3+ charge must be assigned to them, whereas eq 1, with $x = 3$, would result in a 9+ charge. It would thus seem necessary to rewrite the equation of the aquation reaction as



or some equivalent form, which would mean that the polycation is more acidic in the interlayer space than in free solution.

A second remark is that the polycation in the interlayer space would also need to have a lower affinity for the (heidi) ligand: although the equilibrium constants of reactions such as (2) above have not been published, the NMR analysis of solutions indicates that very little uncomplexed Al is present as long as free (heidi) are available.

Finally, we may underline the fact that polycations fill up the interlayer space almost completely. The pillars' density of one pillar per 5 unit cells⁷ is high enough to make the interlayer space inaccessible to N₂ physisorption (the measured BET surface area, 25 m²/g, corresponds only to the external surface of the saponite layers stacks). If the polycations are indeed in close packing, it is understandable that high positive charges would be unfavorable. The question remains of what exactly is the driving force for close packing. In a previous discussion of variable charge saponites pillared by Al₁₃–Keggin polycations,¹⁵ rather similar remarks were made. A maximum of the pillars' density was observed, corresponding to one Al₁₃ pillar per six saponite unit cells. This corresponds to a 2-D close packing if, instead of the radius of the "bare" Al₁₃–Keggin ion, its gyration radius is taken into account (roughly, the radius of the polycation plus its hydration sphere). Two-dimensional steric constraints obviously play an important role in the organization of polycationic pillars during their intercalation between clay layers. In the present case, the formation of the Al₁₃(heidi)₃³⁺ species would result from the competition between heidi ligand affinity for Al³⁺, charge compensation, and steric constraints.

Conclusions

The present results show the ability of 3Q MAS NMR to characterize the structure of nanocomposite materials (pillared

clays) at the molecular level in a case where more classical methods, including 1-D ^{27}Al NMR, failed to provide unequivocal structural elucidation. We reached the conclusion that the Al_{13} -heidi polycations could be intercalated in the interlayer space of saponite clays while keeping their basic structure intact (i.e., with Al coordination and connectivity of Al polyhedra unmodified). However, at a finer level of characterization, it appears that the intercalated polycations have been specifically modified by partial hydrolysis, losing three out of their initial six (heidi) ligands.

The success of our approach was based on a comparison between nanocomposites and a reference bulk salt containing the unmodified polycation. The use of 3Q MAS NMR went beyond this simple fingerprint approach, however, and an analysis of the 2-D signal shape led us to identify the main source of broadening in the spectrum as being due to dipolar interactions rather than to chemical heterogeneity of the intercalated species. This allowed us to choose the model of partial hydrolysis over other hypotheses equally compatible with the information previously available.

It is likely that careful analysis of 3Q MAS ^{27}Al NMR data would permit progress toward the structural understanding of other related nanocomposite materials, provided it is carried out in parallel with more classical determinations (surface area, XRD, elemental analysis, etc.). The integration of macroscopic and molecular (spectroscopic) information is a key factor to success in this program.

The model we propose for Al_{13} -heidi intercalated clays raises interesting questions concerning self-organization in these

systems, for instance, the identification of the driving force for 2-D polycation close packing even in the presence of unfavorable electrostatic interactions. Understanding these phenomena will be necessary to tailor the properties of intercalated and pillared clays of practical importance.

References and Notes

- (1) Lambert, J.-F.; Poncelet, G. *Top. Catal.* **1997**, *4*, 43.
- (2) Plee, D.; Borg, F.; Gatineau, L.; Fripiat, J. J. *J. Am. Chem. Soc.* **1985**, *107*, 2362–2369.
- (3) Medek, A.; Harwood, J. S.; Frydman, L. *J. Am. Chem. Soc.* **1995**, *117*, 12779–12787.
- (4) Man, P. P. In *Encyclopedia of Analytical Chemistry*; Meyers, R. A., Ed.; John Wiley & Sons: Chichester, U.K., 2000; pp 12224–12265 and references therein.
- (5) Vicente, M. A.; Lambert, J.-F. *Phys. Chem. Chem. Phys.* **1999**, *1*, 1633–1639.
- (6) Jordan, P. A.; Clayden, N. J.; Heath, S. L.; Moore, G. R.; Powell, A. K.; Tapparo, A. *Coord. Chem. Rev.* **1996**, *149*, 281–309.
- (7) Heath, S. L.; Jordan, P. A.; Johnson, I. D.; Moore, G. R.; Powell, A. K.; Helliwell, M. J. *Inorg. Biochem.* **1995**, *59*, 785.
- (8) Amoureux, J.-P.; Fernandez, C.; Steuernagel, S. *J. Magn. Reson.* **1996**, *A 123*, 116.
- (9) Man, P. P. *Phys. Rev. B: Condens. Matter* **1998**, *58*, 2764–2782.
- (10) Grandinetti, P. J. <http://www.chemistry.ohio-state.edu/~grandinetti/research/index.html>.
- (11) Brown, S. P.; Wimperis, S. *J. Magn. Reson.* **1997**, *128*, 42–61.
- (12) Vosegaard, T.; Florian, P.; Massiot, D.; Grandinetti, P. J. *J. Chem. Phys.* **2001**, *114*, 4618–4624.
- (13) Klopogge, J. T.; Dirken, P. J.; Geus, J. W.; Jansen, J. B. H. *J. Non-Cryst. Solids* **1995**, *181*, 151–156.
- (14) Massiot, D. *Quadrupolar Interaction*, lecture notes; Ecole de Physique Théorique des Houches, 1997.
- (15) Bergaoui, L.; Lambert, J.-F.; Franck, R.; Suquet, H.; Robert, J.-L. *J. Chem. Soc., Faraday Trans.* **1995**, *91*, 2229.